AD-A189 709 MILITARY HYDROLOGY REPORT 15 THE SEISMIC REFRACTION 1/1
COMPRESSION-SHEAR WAV (U) ARMY ENGINEER WATERWAYS
EXPERIMENT STATION VICKSBURG MS ENVIR
UNCLASSIFIED C SCHUYLER-ROSSIE NOV 87 WES/MP/EL-79-6-15 F/G 17/10 NL

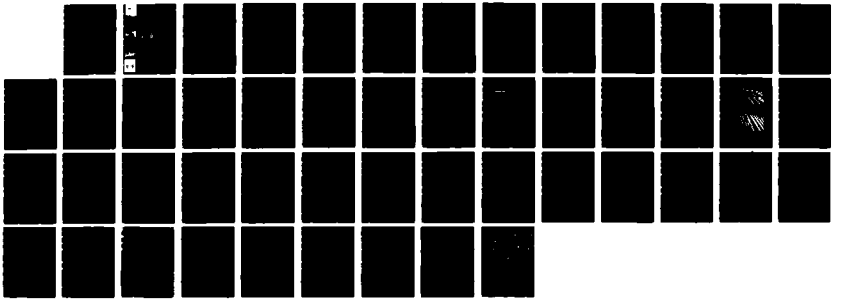

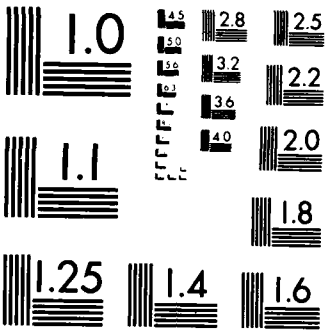

MICROCOPY RESOLUTION TEST CHART
NATIONAL BUREAU OF STANDARDS-1963-A

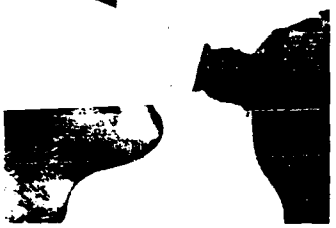

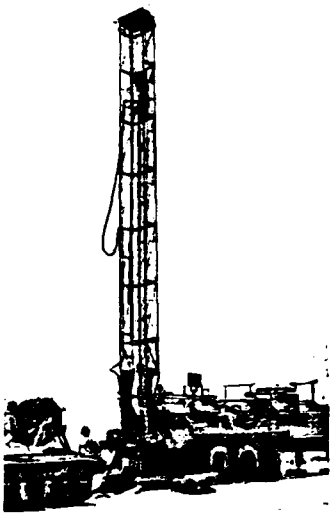

MISCELLANEOUS PAPER EL-79-6

MILITARY HYDROLOGY

Report 15
THE SEISMIC REFRACTION COMPRESSION-SHEAR WAVE VELOCITY RATIO AS AN INDICATOR OF SHALLOW WATER TABLES: A FIELD TEST

by

Christine Schuyler-Rossie

Environmental Laboratory

DEPARTMENT OF THE ARMY
Waterways Experiment Station, Corps of Engineers
PO Box 631, Vicksburg, Mississippi 39180-0631

November 1987
Report 15 of a Series

Prepared for DEPARTMENT OF THE ARMY
US Army Corps of Engineers
Washington, DC 20314-1000

Under DA Project No. 4A762719AT40
Task Area CO, Work Unit 017

MILITARY HYDROLOGY REPORTS

Report No.	No. in Series	Title	Date
TR EL-79-2	-	Proceedings of the Military Hydrology Workshop, 17-19 May 1978, Vicksburg, Mississippi	May 1979
MP EL-79-6 (Military Hydrology Series)	1	Status and Research Requirements	Dec 1979
	2	Formulation of a Long-Range Concept for Streamflow Prediction Capability	Jul 1980
	3	A Review of Army Doctrine on Military Hydrology	Jun 1981
	4	Evaluation of an Automated Water Data Base for Support to the Rapid Deployment Joint Task Force (RDJTF)	Nov 1981
	5	A Quantitative Summary of Groundwater Yield, Depth, and Quality Data for Selected Mideast Areas (U)	Mar 1982
	6	Assessment of Two Currently "Fieldable" Geophysical Methods for Military Ground-Water Detection	Oct 1984
	7	A Statistical Summary of Ground-Water Yield, Depth, and Quality Data for Selected Areas in the CENTCOM Theatre of Operations (U)	Oct 1984
	8	Feasibility of Using Satellite and Radar Data in Hydrologic Forecasting	Sep 1985
	9	State-of-the-Art Review and Annotated Bibliography of Dam-Breach Flood Forecasting	Feb 1985
	10	Assessment and Field Examples of Continuous Wave Electromagnetic Surveying for Ground Water	Jun 1986
	11	Identification of Ground-Water Resources in Arid Environments Using Remote Sensing Imagery	
	12	Case Study Evaluation of Alternative Dam-Breach Flood Wave Models	Nov 1986
	13	Comparative Evaluation of Dam-Breach Flood Forecasting Methods	Jun 1986
	14	Breach Erosion of Earthfill Dams and Flood Routing (BEED) Model	
	15	The Seismic Refraction Compression-Shear Wave Velocity Ratio as an Indicator of Shallow Water Tables: A Field Test	Nov 1987
Unnumbered		Proceedings of the Ground-Water Detection Workshop, 12-14 January 1982, Vicksburg, Mississippi	Dec 1984

Destroy this report when no longer needed. Do not return it to the originator.

The findings in this report are not to be construed as an official Department of the Army position unless so designated by other authorized documents.

The contents of this report are not to be used for advertising, publication, or promotional purposes. Citation of trade names does not constitute an official endorsement or approval of the use of such commercial products.

Unclassified
SECURITY CLASSIFICATION OF THIS PAGE

REPORT DOCUMENTATION PAGE

Form Approved
OMB No. 0704-0188

1a REPORT SECURITY CLASSIFICATION Unclassified	1b RESTRICTIVE MARKINGS
2a SECURITY CLASSIFICATION AUTHORITY	3 DISTRIBUTION / AVAILABILITY OF REPORT Approved for public release; distribution unlimited.
2b DECLASSIFICATION / DOWNGRADING SCHEDULE	
4 PERFORMING ORGANIZATION REPORT NUMBER(S) Miscellaneous Paper EL-79-6	5 MONITORING ORGANIZATION REPORT NUMBER(S)
6a NAME OF PERFORMING ORGANIZATION USAEWES Environmental Laboratory 6b OFFICE SYMBOL (If applicable)	7a NAME OF MONITORING ORGANIZATION
6c ADDRESS (City, State, and ZIP Code) PO Box 631 Vicksburg, MS 39180-0631	7b ADDRESS (City, State, and ZIP Code)
8a NAME OF FUNDING / SPONSORING ORGANIZATION US Army Corps of Engineers 8b OFFICE SYMBOL (If applicable)	9 PROCUREMENT INSTRUMENT IDENTIFICATION NUMBER Contract No. DACA39-85-M-1166 See reverse
8c ADDRESS (City, State, and ZIP Code) Washington, DC 20314-1000	10 SOURCE OF FUNDING NUMBERS PROGRAM ELEMENT NO. / PROJECT NO. / TASK NO. / WORK UNIT ACCESSION NO.

11 TITLE (Include Security Classification)
Military Hydrology; Report 15, The Seismic Refraction Compression-Shear Wave Velocity Ratio as an Indicator of Shallow Water Tables: A Field Test

12 PERSONAL AUTHOR(S)
Schuyler-Rossie, Christine

13a TYPE OF REPORT	13b TIME COVERED	14 DATE OF REPORT (Year, Month, Day)	15 PAGE COUNT
Report 15 of a series	FROM _____ TO _____	November 1987	45

16 SUPPLEMENTARY NOTATION
Available from National Technical Information Service, 5285 Port Royal Road, Springfield, VA 22161.

17 COSATI CODES		
FIELD	GROUP	SUB-GROUP

18 SUBJECT TERMS (Continue on reverse if necessary and identify by block number)
Compression, Military hydrology, Shear wave velocity, Geophysics, Seismic refraction, Wave velocity, Ground water

19 ABSTRACT (Continue on reverse if necessary and identify by block number)

To test the assumption that the velocity of shear waves increases much less than the velocity of compressional waves at a water table, a seismic refraction survey was performed over a shallow water table in alluvial sediment. Using a sledge hammer and a partially buried steel cylinder as a source, a maximum shot-to-receiver distance of 330 ft and depth of investigation of 60 ft were achieved. The ratio of V_p to V_s (compressional/shear wave velocity) at the water table was found to be 2.48. In the four nonsaturated layers above the water table, V_p/V_s ratios ranged from 1.54 to 1.55. As predicted by the theoretical models considered, shear wave velocity did not increase measurably at the water table. In an area in which a shallow water table was not likely to exist, shear wave velocity increased by at least as much as the increase in compressional velocity at each refractor. Results indicate that the comparison of S- and P-wave velocity profiles is a promising technique for water table detection. However, more research is necessary to define the reliability and limits of the method.

20 DISTRIBUTION / AVAILABILITY OF ABSTRACT	21 ABSTRACT SECURITY CLASSIFICATION
☒ UNCLASSIFIED/UNLIMITED ☐ SAME AS RPT ☐ DTIC USERS	Unclassified
22a NAME OF RESPONSIBLE INDIVIDUAL	22b TELEPHONE (Include Area Code) / 22c OFFICE SYMBOL

DD Form 1473, JUN 86 *Previous editions are obsolete*

SECURITY CLASSIFICATION OF THIS PAGE
Unclassified

10. SOURCE OF FUNDING NUMBERS (Continued).

DA Project No. 4A762719AT40,
Task Area CO, Work Unit 017

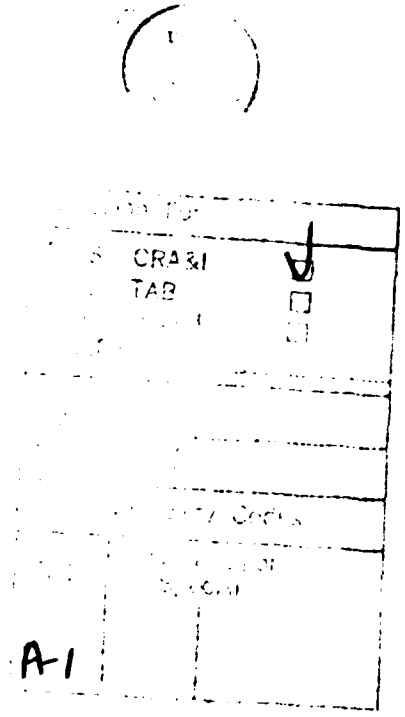

PREFACE

This work was performed during the period August 1985 to January 1986 by Ms. Christine Schuyler-Rossie, a contract student at the Colorado School of Mines (CSM), Golden, Colo., under Contract No. DACA39-85-M-1166 with the US Army Engineer Waterways Experiment Station (WES). This report is essentially a thesis submitted to the Graduate School of CSM in partial fulfillment of the requirements for the Master of Science Degree in the Department of Geophysics.

Acknowledgment is made to Dr. Phillip R. Romig, Professor and Head, Department of Geophysics, who served as faculty advisor during the preparation of the thesis; to Committee members, Drs. Thomas L. Dobecki and Catherine Skokan, Department of Geophysics, CSM, who provided technical guidance during the course of study; and to Mr. Michael Powers, graduate student, Department of Geophysics, CSM, who developed software (including TRANDEC and DISPICK) that was used to transfer field data from magnetic tape to the IBM personal computer.

The effort was funded by the Office, Chief of Engineers (OCE), US Army, under Department of the Army Project No. 4A762719AT40, "Mobility, Soils and Weapons Effects Technology," Task Area CO, Work Unit 017, "Remote Procedures for Locating Water Supplies." Mr. Austin A. Owen was the OCE Technical Monitor.

Principal Investigators of Work Unit 017 are Messrs. Elba A. Dardeau, Jr., and John G. Collins, Environmental Constraints Group (ECG), Environmental Systems Division (ESD), Environmental Laboratory (EL). The work unit was conducted under the general supervision of Mr. Malcolm P. Keown, Chief, ECG; Dr. Lewis E. Link, Jr., Chief, ESD; and Dr. John Harrison, Chief, EL. The Chief of ESD during preparation and publication of this report was Dr. Victor E. LaGarde. This report was edited by Ms. Jessica S. Ruff of the WES Information Technology Laboratory.

COL Allen F. Grum, USA, was the previous Director of WES. COL Dwayne G. Lee, CE, is the present Commander and Director. Dr. Robert W. Whalin is Technical Director.

This report should be cited as follows:

Schuyler-Rossie, C. 1987. "Military Hydrology; Report 15: The Seismic Refraction Compression-Shear Wave Velocity Ratio as an Indicator of Shallow Water Tables: A Field Test," Miscellaneous Paper EL-79-6, US Army Engineer Waterways Experiment Station, Vicksburg, Miss.

CONTENTS

	Page
PREFACE	1
CONVERSION FACTORS, NON-SI TO SI (METRIC) UNITS OF MEASUREMENT	4
PART I: INTRODUCTION	5
Background	5
Objectives and Scope	6
PART II: THEORY	8
PART III: METHOD	12
Survey Sites	12
Energy Sources	13
Recording Equipment and Spread Description	17
Data Processing and Analysis	19
PART IV: RESULTS AND DISCUSSION	20
Source Characteristics	20
Characteristics of Shear Velocity and Velocity Ratio	20
PART V: CONCLUSIONS AND RECOMMENDATIONS	28
Conclusions	28
Recommendations	28
REFERENCES	31
APPENDIX A: UNCONSOLIDATED GRANULAR MEDIUM MODEL	A1
APPENDIX B: TIME-DISTANCE PLOTS AND TRAVEL TIME DATA	B1

CONVERSION FACTORS, NON-SI TO SI (METRIC)
UNITS OF MEASUREMENT

Non-SI units of measurement used in this report can be converted to SI (metric) units as follows:

Multiply	By	To Obtain
feet	0.3048	metres
inches	2.54	centimetres
miles (US statute)	1.609347	kilometres
pounds (mass)	0.4535924	kilograms

MILITARY HYDROLOGY

THE SEISMIC REFRACTION COMPRESSION-SHEAR WAVE VELOCITY RATIO AS AN INDICATOR OF SHALLOW WATER TABLES: A FIELD TEST

PART I: INTRODUCTION

Background

1. Military hydrology is a specialized field of study that deals with the effects of surface and subsurface water on the planning and conduct of military operations. In 1977, the Office, Chief of Engineers, approved a military hydrology research program; management responsibility was subsequently assigned to the Environmental Laboratory, US Army Engineer Waterways Experiment Station (WES), Vicksburg, Miss.

2. The objective of military hydrology research is to develop an improved hydrologic capability for the Armed Forces with emphasis on application in the tactical environment. To meet this overall objective, research is being conducted in four thrust areas: (a) weather-hydrology interactions, (b) state of the ground, (c) streamflow, and (d) water supply.

3. Previously published Military Hydrology reports are listed on the inside of the front cover. This report is the sixth that contributes to the water-supply thrust area, which is oriented toward the development of an integrated methodology for rapidly locating and evaluating ground-water supplies, particularly in arid regions. Specific work efforts include: (a) the compilation of guidelines for the expedient location of water for human survival, (b) the development of remote imagery interpretation procedures for detecting and evaluating ground-water sources, (c) the adaptation of suitable geophysical methods for detecting and evaluating ground-water sources, and (d) the development of water-supply analysis and display concepts.

4. Water supply, particularly in arid regions, has been identified as a high-priority problem for the military. Surface water supplies are inadequate, unreliable, and unpredictable in many arid regions of strategic importance; thus, the capability of detecting producible ground-water resources in

such areas is critically important. However, technology shortfalls exist in surface techniques for detection of ground water.

5. A Ground-Water Detection Workshop was held in Vicksburg, Miss., in January 1982 to consider, among other topics, the technology shortfalls in surface techniques for detection of ground water. The conclusions of the Geophysics Working Group at the Workshop were: (a) two currently fieldable geophysical methods (electrical resistivity and seismic refraction) are applicable to the ground-water detection problem and may offer a near-term solution to the technology shortfall, and (b) several state-of-the-art and emerging geophysical techniques may have potential for the long-term solution. This report presents the results of field tests conducted in Colorado in which seismic compressional V_p or longitudinal (P-wave) and shear wave (S-wave) velocities V_s were compared for detection of the water table. Even though seismic refraction is considered a currently fieldable method, the V_p/V_s approach is considered new and innovative.

6. The seismic refraction method is often used to help map water table levels. However, the compressional wave velocity commonly used in refraction surveys varies with both rock type and fluid saturation. Thus, changes in lithology and changes in saturation are difficult to distinguish when using P-wave velocities alone.

7. Theoretically, S-wave velocity decreases or increases only slightly, while P-wave velocity increases sharply at a water table refractor, suggesting that a comparison of V_p/V_s ratios over a refraction profile could be used to detect a water table. Some obstacles to using this technique are the difficulty of generating shear wave first arrivals and the lack of previous research on the actual change in velocity of refracted shear waves at a real water table.

Objectives and Scope

8. To test this method under real field conditions, the refraction survey described herein was performed on the western edge of the San Luis Valley, Colorado, in May and June 1985. The goals of the study were to:

a. Find a combination of equipment and procedures capable of generating and recording good quality, easily identifiable shear wave first arrivals.

b. Obtain evidence of the actual behavior of V_s at a water saturation boundary under real field conditions.

A steel cylinder struck with a hammer and a wooden plank struck with a hammer were the two shear wave sources tested. Using the cylinder source, the V_p/V_s ratio was measured in a reversed refraction profile over a shallow water table.

PART II: THEORY

9. The method described herein applies to the detection of water table aquifers only. Confined aquifers, in which water is confined under pressure in a porous rock layer between two layers of low permeability, are not suitable targets for seismic refraction surveys. According to Snell's law, a critical refraction along a boundary occurs only when a wave travels from a lower to a higher velocity medium. Because the low-permeability confining layer above a confined aquifer often has a higher seismic wave velocity than the underlying aquifer, no critical refraction occurs at the associated aquifer surface, and the confined aquifer acts as a hidden layer in the velocity analysis.

10. In an unconfined water table aquifer (Figure 1), the water level is not determined by a confining layer directly above the aquifer. There need be no change in lithology at the water surface. Instead, the water table surface

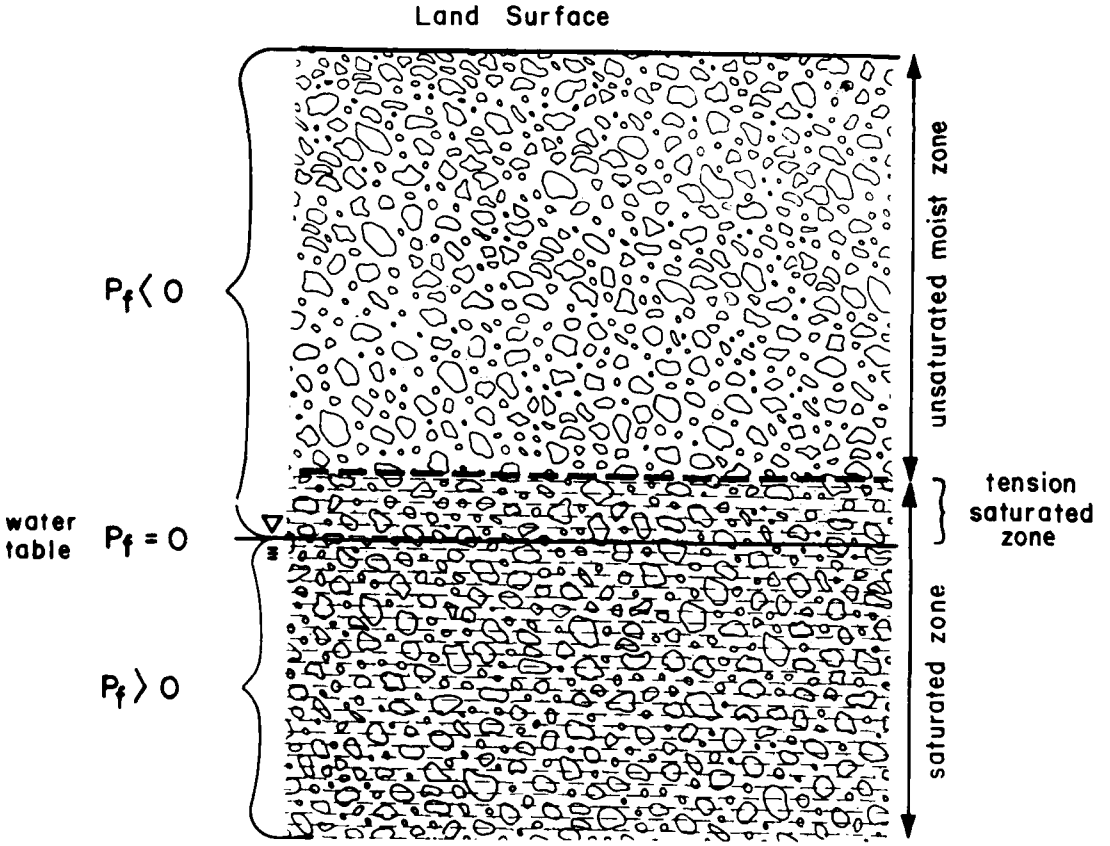

Figure 1. Water table in uniform unconsolidated medium

is at atmospheric pressure, just as water standing in an open container would be. The water table is defined as the level at which the fluid pressure P_f of the water measured in gauge pressure (that is, with respect to atmospheric pressure) is exactly zero (Freeze and Cherry 1979). Below the water table, the medium is completely saturated, and the pore spaces are completely filled with water. Above the water table, there are two zones--a narrow capillary zone of saturation in which the pores are filled with water at negative pressures, i.e., under tension, and above that an unsaturated zone where some pores are filled with water at negative fluid pressures and some with air. At and below the water table, pore water pressures influence the elastic parameters of the medium and can change the velocity of waves traveling through the medium.

11. The velocity of P-waves is given by:

$$V_p = \sqrt{\frac{(3k + 4\mu)}{\rho}} \tag{1}$$

where

k = bulk modulus

μ = shear modulus or rigidity of the material in which the wave is traveling

ρ = density

The velocity of shear waves is

$$V_s = \sqrt{\frac{\mu}{\rho}} \tag{2}$$

A ground-water aquifer essentially consists of a skeleton or framework of solid material and pore spaces filled with a fluid such as air or water. The solid material comprising the framework has a certain bulk modulus, rigidity, and density. When this material is arranged in a porous framework, the resulting skeleton has its own values of k, μ, and ρ that differ from the values of these parameters in the pure solid material. The fluid that fills the pore spaces also has a distinct bulk modulus and density. Unlike the solid framework, however, the fluid has a rigidity of zero. The parameters k, μ, and ρ of the whole lithologic unit depend on the individual parameter values of the skeleton and the pore fluid. Because the shear

modulus is zero for all fluids including air and water, the overall rigidity of the lithologic unit is independent of the type of fluid that fills the pore spaces.

12. When air in pores is replaced by water, the overall bulk modulus increases significantly, while density increases to a lesser degree; rigidity, however, is not significantly affected. Because P-wave velocity depends on k, μ and ρ, while S-wave velocity depends only on μ and ρ, one expects a greater change in V_p than in V_s when a wave travels from an unsaturated moist zone to a water-saturated medium. Because the density of water is greater than that of air, and velocity is inversely proportional to the square root of density, the velocity of shear waves should decrease somewhat at a water table refractor rather than increase as P-wave velocity does. Assuming that the secondary effects of water on the framework rigidity (e.g., framework softening due to wetting or framework stiffening due to precipitation and encrustation of solutes) are negligible, a comparison of compressional and shear wave refractions over the same seismic line could be useful in both distinguishing a water table from a change in lithology and determining the depth to the water table.

13. When a water table occurs within an unconsolidated lithologic unit, P-wave velocity increases, usually by 2,000 or 3,000 ft/sec, at the water table (Eaton 1974, Levshin 1961). According to calculations based on a theoretical model of an unconsolidated granular medium (Levshin 1961), this increase is sharp. If S-wave velocity decreases or remains the same at this boundary, there would be no S-wave critical refraction at the water table. A comparison of V_p to V_s at this depth would show that the sharp increase in V_p is probably due to water saturation rather than lithologic change. On the other hand, if both V_p and V_s increase sharply at a given depth, the boundary is probably indicative of a change in lithology rather than just a water table. Even though V_p may be in the right range for a compressional wave in saturated soil, about 5,000 ft/sec, a marked change in V_s would indicate a lithology change.

14. Although most water tables occur in unconsolidated or poorly consolidated sediments, many investigations of the behavior of shear waves in saturated media have focused on consolidated sediments or fractured crystalline rock. For example, according to calculated wave velocities in theoretical models of saturated and dry rocks (Kuster and Toksoz 1974), the

variability of V_p is 4 to 10 times greater than that of V_s when air in pore spaces is replaced by water. The larger contrast is for a typical sandstone model and the smaller for a fractured crystalline rock model.

15. Shallow seismic exploration for ground water often occurs in unconsolidated or poorly consolidated sediments, and the V_p/V_s values calculated by Kuster and Toksoz (1974) refer to consolidated sandstone or fractured crystalline rock; therefore, a model that is more representative of actual conditions should be considered. Results from a granular medium model based on an assumption of cubic packing of ideally elastic spheres (White and Sengbush 1953) suggest that V_s decreases in proportion to $1/\rho$ at a water saturation boundary and that the maximum change in V_s is not more than 15 percent (Levshin 1961). However, this same model, described in Appendix A, predicts a sharp change in V_p, a change that is most pronounced at depths of less than 165 ft where the velocity above the water table would usually be low.

16. Although much is known about the behavior of refracted P-waves at saturation boundaries, less is understood about refracted S-waves. There are two reasons for the relative lack of knowledge of S-wave behavior. First, P-waves are easier to generate using explosives or other impulsive sources. Second, compressional wave velocity is always greater than shear wave velocity in a given medium; therefore, P-waves arrive at the receivers ahead of S-waves and interfere with the determination of first arrival times of shear waves.

17. Because little is known about the actual changes in shear wave velocity at a water table, V_s cannot be assumed to decrease as predicted by the theoretical models considered thus far. The values for V_s can possibly increase slightly at a saturation boundary. When fluid is enclosed in small pore spaces and particle motion is at low frequencies, the viscosity of the pore fluid may allow the transmission of a small amount of shear motion (Biot 1956, White 1983). At a water saturation boundary, V_s can change in proportion to the change in pore fluid viscosity as well as the change in density. However, even though fluid rigidity is not necessarily constant in this case, the increase in μ would be very small in comparison with the increase in k at a water saturation boundary. Thus, V_s can be expected to increase slightly at a water table, in some cases, but not nearly as sharply as V_p.

PART III: METHOD

Survey Sites

18. A seismic survey was conducted on land owned by the State of Colorado in Section 1 of Range 6E, Township 40N, on the western edge of the San Luis Valley in Rio Grande County (Figure 2). The San Luis Valley is at the northern end of the Rio Grande Rift and is bounded on the east by the Sangre de Cristos, which are fault block mountains, and on the west by volcanic hills and ridges. The valley is filled with alluvial sediment

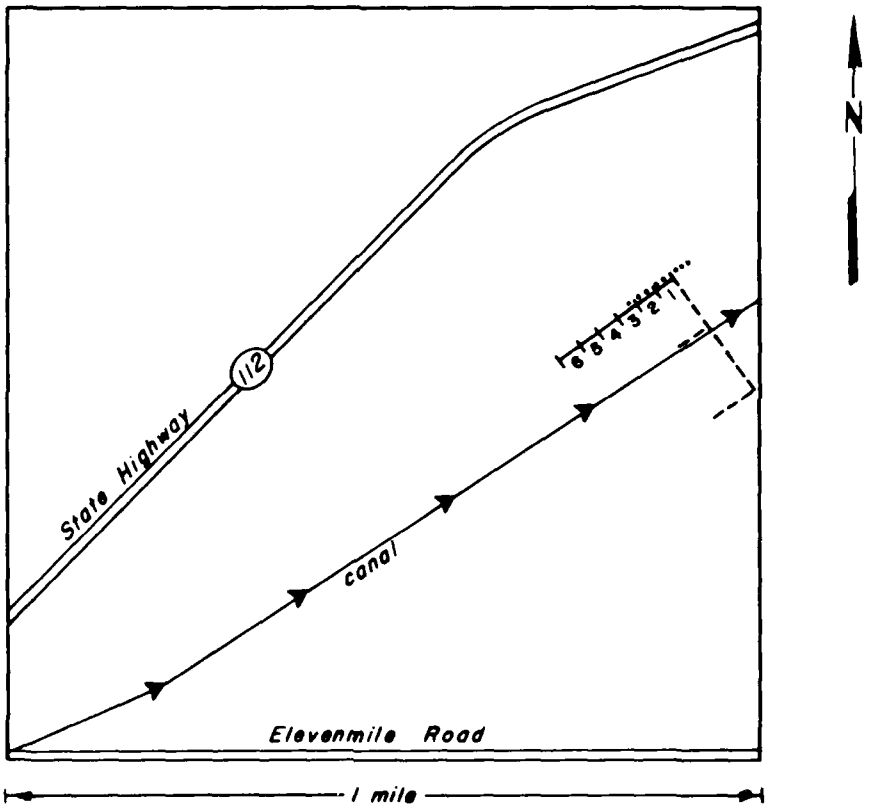

NOTE: THE TEST SPREADS WERE PRELIMINARY HAMMER LINKS TO DETERMINE GEOPHONE SPACING AND SHOT-TO-SHOT DISTANCES

Figure 2. Area 1 survey location

interlayered on the west with occasional ash and lava flows. The near subsurface of the survey area consists of unconsolidated to poorly consolidated gravelly alluvium. The depth to the nearest igneous unit, estimated trigonometrically from the distance and dip of a nearby outcrop, is 500 ft, well below the range of this investigation.

19. An unlined irrigation canal flowing southwest to northeast through the area is a probable recharge source for the near-surface water table. Due to limitations of the source energy and the spread lengths* used, a water table depth of not more than 50 ft was desired to get an estimate of V_s at the water table. Because the water table was likely to be higher near the canal, the seismic line (Area 1) was placed parallel to and about 220 ft from the northwest side of the canal. Prior to the survey parallel to the canal, some test configurations using various sources and spread lengths were carried out at different locations in the same area, as shown in Figure 2.

20. After completion of the Area 1 survey, an additional line, Area 2, was surveyed in the hills to the west, specifically in Section 2, Range 4E, Township 40N, in Rio Grande County, Colorado (Figure 3). Area 2 consists of a thin soil layer over volcanic bedrock. Other researchers there had located a 15- to 20-ft-deep layer with a compressional wave velocity between 4,000 and 6,000 ft/sec. A comparison of V_p to V_s at this location was needed to determine if this layer was a water saturation zone or weathered bedrock.

Energy Sources

21. Continuous energy sources, such as commercial shear vibrators, were not employed in this study for several reasons. First, layers that must be identified in ground-water exploration are usually shallow and thin compared with those of interest in deep reflection seismology for which commercial shear vibrators were designed. At the velocities usually encountered in shallow exploration, a maximum frequency of 100 Hz in a vibrator sweep results in a minimum wavelength of 30 ft. Because the thicknesses or the depths of many layers of interest are less than 30 ft, this type of source often cannot provide the necessary resolution for such a survey. Second, this equipment is

---

* Distance from source to last geophone or length of seismic refraction line.

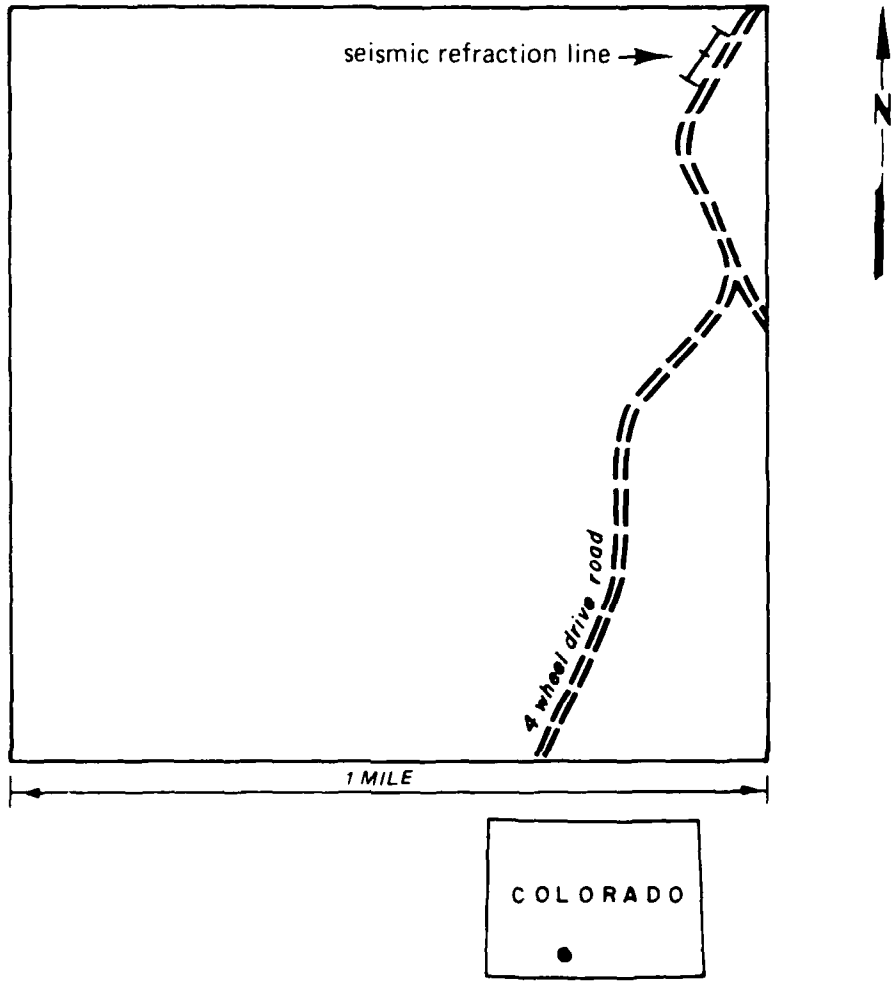

Figure 3. Area 2 survey location

expensive, and many of the consultants or small companies working in engineering or ground-water geophysics cannot afford the equipment. Third, vibrators are large, heavy, and difficult to maneuver and so cannot be easily operated on sites where access is limited. Finally, the records generated by continuous sources require extensive data processing. Large-capacity computers are expensive, and commercial processing services are usually designed for deep reflection processing. The information from shallow depths, of interest to the engineering geophysicist, is often treated as noise and muted in commercial processing.

22. An impulse source is better suited than vibrational sources to meeting the needs of engineering geophysicists engaged in ground-water exploration. However, the lack of high-energy impulse sources that generate only transverse waves is a major obstacle to the common use of shear refraction surveys.

23. For impulsive sources that employ a target struck with a hammer, there are two mechanisms by which unwanted P-waves are generated. First, striking source materials for which Poisson's ratio is not zero results in contraction in the direction of transverse particle motion. This action, in turn, results in expansion in the direction of wave propagation and the generation of some compressional motion along the line of receivers. Second, any component of motion of the hammer toward the receivers sends stray compressional energy along the receiver line. Because the compressional wave velocity is always greater than the shear wave velocity, the compressional wave first arrival reaches the geophones ahead of the shear wave. Often the P-wave is still passing the receiver when the shear wave arrives. Separating the shear wave arrival from the passing compressional wave is often difficult, if not impossible. Even when horizontal geophones are used, P-waves from shallow layers arrive at a low angle to the surface with enough horizontal component of motion to obscure the shear record.

24. To obtain identifiable shear first arrivals, a source that minimizes compressional wave generation must be chosen, and full advantage must be taken of the polarization of shear waves. Horizontal shear waves (SH) are preferable for this type of application because they do not convert to compressional or vertical shear at planar refraction boundaries. (This assumes that the seismic line runs along the dip direction of any inclined layers.) Various attempts to develop surface shear sources are described in the literature (Applegate 1974; Gibson, Boomer, and Schoellhorn 1979; Won 1980). The methods most readily available, reliable, and inexpensive consist of some object driven, buried, or weighted into the ground and struck with a hammer in a horizontal direction normal to the receiver line. The shear motion that is produced can be detected by horizontal geophones placed with their sensitive axes normal to the line. When such a source is struck to the left, the first motion at the geophone is to the left, whereas first motion is to the right if the source is struck to the right. This mode of propagation is referred to as "shear wave polarity." If two traces of opposite polarity are added, the

shear wave arrivals will tend to cancel each other, but the P-wave signal will be enhanced. However, if the polarity of one of the traces is reversed at the seismograph, and the two traces are added, the P-waves will tend to cancel and the shear signal will be enhanced. This procedure can be used to suppress the P-wave arrivals enough to obtain identifiable first arrivals for the shear wave.

25. For this study, two shear sources were tried. Both involved the use of a sledge hammer and either a piezoelectric trigger on the handle or a trigger geophone set close to the source to start the seismograph when the hammer struck the target. The first source was a large wooden beam struck on end with the hammer. Coupling with the ground was improved by placing the front wheels of a truck on the beam. The second source was a 3.5-in.-diam, 1-ft-long steel cylinder. One end of the cylinder was seated in a shallow ramp dug into the earth (Figure 4) with the opposite end protruding above the ground surface. The protruding end was struck with a hammer, causing the other end to impact the ground at the end of the trench. The signal was improved by placing a small steel plate at the lower end of the ramp between the cylinder and the ground. Of these two sources, the steel cylinder gave a clearer, stronger shear signal and also was more likely to start the trigger geophone or hammer trigger at first impact, probably because of better coupling. Whereas the cylinder was seated in the ground, the wooden plank was only weighted down onto the soil surface; therefore, the shear wave from the plank was transmitted through friction in very loose topsoil. Because accurate zero times were critical to the process of adding together reversed polarity traces to subdue the P-waves, the steel cylinder was used throughout the survey.

26. To obtain V_p for comparison with V_s, the cylinder was placed vertically into the ground with one end above the surface and struck vertically with the hammer. For both P- and S-waves, 2 to 10 hammer blows were stacked together to obtain a readable amplitude signal at all geophones. Hammer blows were taken on both ends of each spread to obtain reverse refraction profiles so that true velocities and refractor dip angles could be calculated from the apparent velocities and intercept times from each shot position. In addition to the hammer blows, one section of the line was shot with 1/3-lb Kinepac explosive.

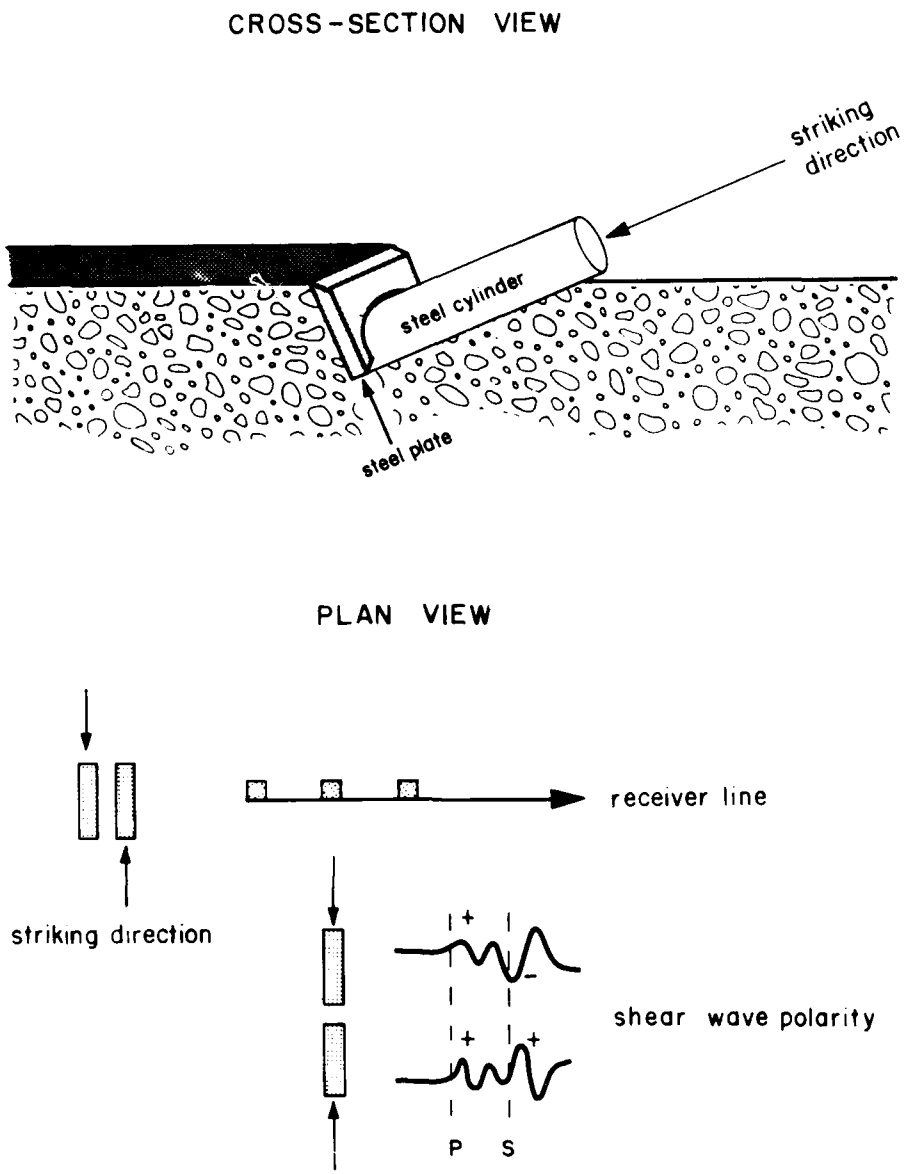

Figure 4. Shear wave source

Recording Equipment and Spread Description

27. Mark Products low-frequency horizontal geophones were used as shear receivers. Twelve of these were placed with the sensitive axes normal to the line. Care was taken to center the level bubble on each geophone and to face the positive polarity end of each axis in the same direction so that the direction of first motion would be the same on all 12 traces. The P-wave receivers were Mark Products low-frequency vertical geophones. A pair of

geophones, one horizontal and one vertical, was placed at each receiver station, and the appropriate geophone was plugged into the cable for recording each type of wave. All 12 geophones were buried approximately 6 in. deep in the soil to reduce wind noise.

28. Two different 12-channel digital seismographs were used. One, a Bison 8012A, allowed the operator to reverse the polarity of the incoming signal by means of a pushbutton on the keyboard. The other seismograph used, a Geometrics 1210F, did not have a polarity reversal capability; however, it had greater gain capacity, which enhanced the signal recorded from the far geophones. Polarity reversal was achieved by a patch panel with the Geometrics seismograph. Both seismographs had compatible magnetic tape recorders that were used to store the traces recorded in the field.

29. Various geophone spacings and spread lengths were tried in the pre-survey tests. To achieve the maximum possible depth of investigation, the longest spread length that could be used and that would reliably produce usable shear records had to be determined. On the other hand, geophone stations had to be close enough together so that several velocity layers could be resolved on the time-distance plots. A spread length of 165 ft and a receiver spacing of 15 ft, which proved to be the best combination, was used throughout the survey along the canal. Shots were taken at 15- and 165-ft offsets from each end of each spread, so that the maximum shot-to-receiver distance was 330 ft. The line parallel with the canal consisted of six spreads. The last receiver station of one spread became the first receiver location of the next spread, resulting in a total line length of 990 ft from the first to last receiver station.

30. In addition, over the first part of the line (northeast end), a 550-ft spread with 50-ft geophone spacings was shot using explosives. Only compressional waves were recorded from this spread. The shots were 50 ft from each end, resulting in a maximum shot-to-receiver distance of 600 ft. For the line in Area 2 (Figure 3), geophone spacing was 10 ft with shots at 10- and 110-ft offsets. Two such spreads were completed for a total line length of 220 ft from first to last geophone station.

Data Processing and Analysis

31. Travel time picks* were made in the field from both the CRT screen on the Bison and printed records from the Geometrics seismograph. Appendix B contains time-distance plots and travel time data tables for all spreads from both lines. Most of the data from the two lines were stored on magnetic tape on the Geometrics-compatible reel-to-reel recorder. Using TRANDEC software developed at the Colorado School of Mines (CSM), these traces were transferred to diskette for use with an IBM personal computer (PC). DISPICK, another program that allows these traces to be displayed, enhanced, and picked on the PC monitor screen, improved the accuracy of arrival times that were difficult to pick from field records. Apparent velocities and intercept times were identified on time-distance plots. A computer program for analysis of multiple dipping planar layers (Mooney 1984) adapted for a Texas Instruments Professional PC was used to calculate depths, dip angles, and true velocities of the layers from the apparent velocities and intercept times.

---

* Identification of the arrival time of a seismic wave.

PART IV: RESULTS AND DISCUSSION

Source Characteristics

32. The first objective of this investigation was to find a practical method for producing good quality shear wave first arrivals; this objective was clearly met by the source and recording procedures used. Figure 5 shows some typical shear records obtained during this investigation. Though the compressional components are not zero on every trace, they are of low enough amplitude that the shear first arrivals are easily visible as up breaks in Figure 5a and down breaks in Figure 5b.

33. The primary limitation of the source used was signal strength. Because of this limitation, the spread length and shot-to-receiver distances that could be used were shorter than the usual lengths for explosive sources. This, together with the inherently slow velocities of shear waves, meant that no shear refractions from deeper than 60 ft could be accurately detected.

Characteristics of Shear Velocity and Velocity Ratio

Area 1 refraction results

34. Analysis of the travel time curves for Area 1 resulted in the velocities and intercept times shown in Tables 1 and 2. An analysis of multiple dipping layers using an unnamed program developed by Mooney (1984) resulted in the models of compressional and shear wave velocity structure shown in Figure 6.

35. The analysis shows that at a depth of 50 to 65 ft there was a layer with a compressional velocity of 5,967 ft/sec. Surface compressional velocity is 869 ft/sec, and intermediate layers have velocities of 2,365 and 3,711 ft/sec. In the center of the line, an additional layer with a V_p of 1,316 ft/sec was detected.

36. The highest V_p layer, 5,967 ft/sec, is within the expected range of compressional velocities for saturated soil and was probably indicative of a water table. The change in V_p at this boundary is 2,256 ft/sec, an increase of 61 percent. The actual difference in the indicated water level was less than 15 ft over a horizontal distance of nearly 1,000 ft. The rise in the water table level at the northeast end was possibly due to the fact

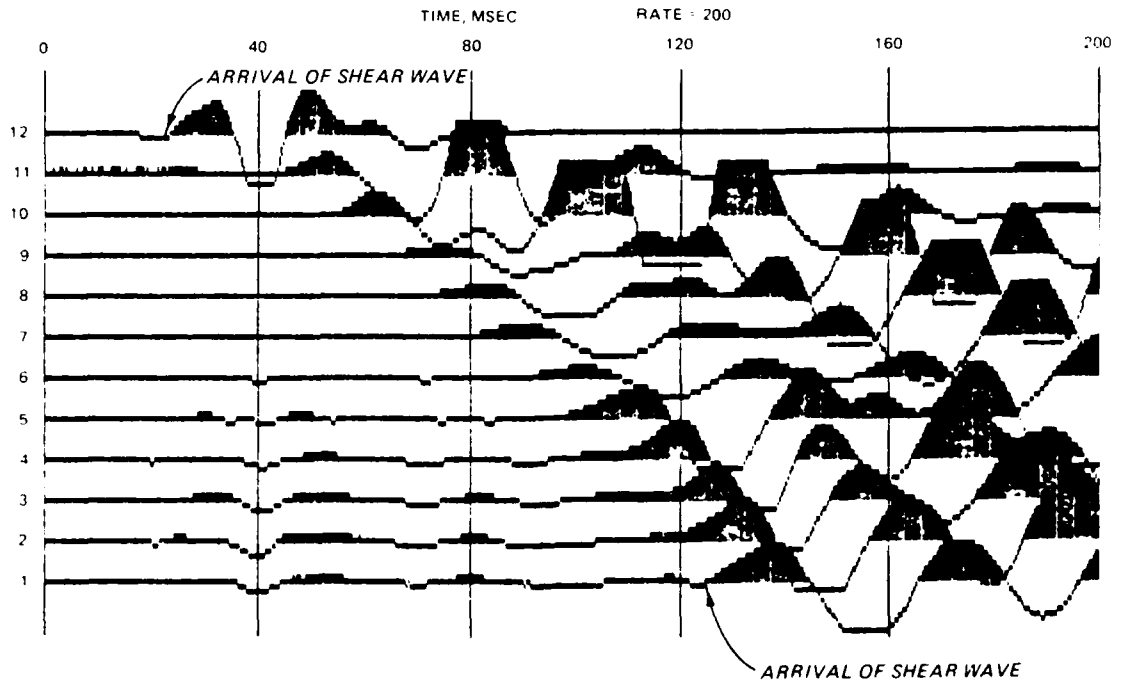

a. From 15-ft offset shot

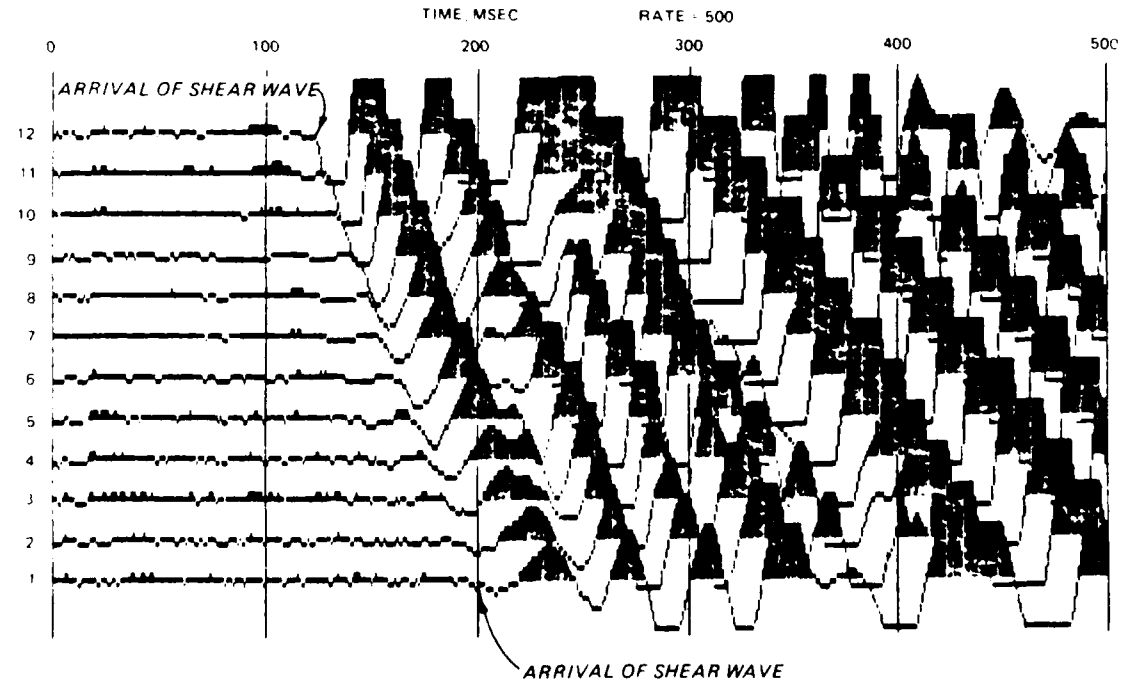

b. From 165-ft offset shot

Figure 5. Sample shear wave record

Table 1

Area 1 Apparent Shear Velocities and Intercept Times (Velocities in feet per second, Times t_0 in milliseconds)

Spread	Layer	Northeast velocity, t_0	Southwest velocity, t_0
1-S	1	667	682
	2	1,696, 29	1,696, 26
	3	2,171, 55	2,500, 67
2-S	1	600	600
	2	1,535, 28	1,611, 20
	3	2,532, 54	2,500, 50
3-S	1	536	600
	2	1,466, 21	1,466, 21
	3	2,053, 37	2,619, 46
4-S	1	600	600
	2	833, 5	882, 9
	3	1,875, 39	1,950, 35
	4	2,340, 52	2,191, 46
5-S	1	500	500
	2	1,318, 20	1,291, 17
	3	2,340, 46	2,268, 57
6-S	1	441	584
	2	1,598, 28	1,625, 29
	3	2,340, 52	2,705, 60

that the ground surface immediately to the northeast of the line was flooded to a depth of several inches. This area could have been acting as an additional recharge source to the water table in the adjacent area. There was, however, no indication at the surface of any additional local recharge source to the southwest that would account for the rise of the water table level at that end of the line.

37. The possibility should be considered that an increase in V_s, and thus a refraction of the SH wave, did occur at the water table but was not seen on the time-distance plots. This could occur if V_s was too low in relation to the boundary depth and spread length to arrive at the far receivers ahead of the refractions from a shallower boundary. REFRMOD

Table 2

Area 1 Apparent Compressional Velocities and Intercept Times

(Velocities in feet per second, times t_0 in milliseconds)

Spread	Layer	Northeast velocity, t_0	Southwest velocity, t_0
1-P	1	1,154	750
	2	2,468, 15	2,617, 25
	3	3,979, 34	3,611, 32
	4	6,346, 56	5,322, 47
2-P	1	937	555
	2	2,045, 10	2,191, 8
	3	3,679, 21	3,679, 23
	4	5,909, 44	6,250, 49
3-P	1	937	1,250
	2	2,167, 9	2,143, 10
	3	4,230, 35	3,703, 27
	4	5,964, 40	6,781, 50
4-P	1	937	937
	2	1,500, 1	1,579, 6
	3	2,437, 9	2,746, 16
	4	3,611, 21	3,823, 23
	5	5,909, 45	6,428, 50
5-P	1	937	937
	2	2,671, 13	2,321, 6
	3	3,250, 18	3,611, 25
	4	5,823, 45	5,439, 39
6-P	1	937	
	2	2,321, 15	2,267, 13
	3	3,823, 30	3,823, 29
	4	5,909, 45	4,853, 32
Explosive-P	1	1,428	1,087
	2	3,846, 28	3,703, 27
	3	5,856, 42	6,250, 49

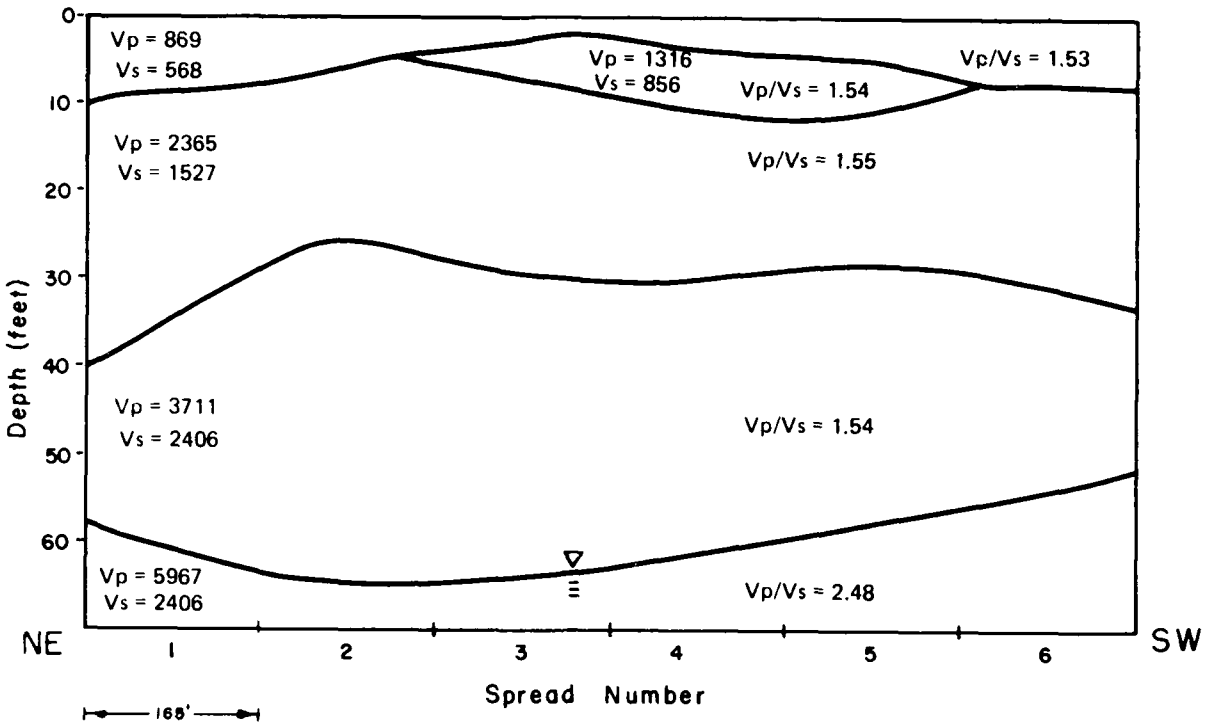

Figure 6. Area 1 velocity profile (velocities in feet per second)

(developed by Dr. Phillip R. Romig, CSM), a computer program that generates simulated time-distance plots from a given velocity, depth, and spread length model was used. Assumed values of V_s were input to the model. When V_s values 10 percent or greater than V_s above the water table (unsaturated condition) were used, the result was apparent in the simulated plots and unlike the actual time-distance plots. V_s was, therefore, assumed to have increased by no more than 10 percent at the water table because no such velocity segment was recorded in the actual plots. Because V_p increased by 61 percent at the water table, the increase, if any, in V_s could not have been very large in comparison to the change in V_p at that boundary.

38. If the layer with a V_p of 5,967 ft/sec is indeed a water table, V_s would not be expected to increase sufficiently to result in critical refraction at the water table. The V_p/V_s ratios in the layers above the water table are 1.55, 1.54, 1.55, and 1.54 from the surface down, while the ratio at the water table is 2.48, an increase of 61 percent.

39. There were no onsite well data to confirm the water table level; consequently, the possibility that the 5,927-ft/sec layer was not a water saturation boundary, but rather some other change in the subsurface that affected

compressional velocity more than shear velocity, had to be considered. However, the velocity analysis from the 550-ft spread shot with explosives at the southwest end of the line indicated that V_p was within the range for water-saturated soils to a depth of at least 70 ft. There was no indication from the explosive spread of additional deeper layers. Because an elevated water table likely exists near the canal, there is a good probability that the boundary at 55 to 65 ft was, in fact, a water saturation boundary.

40. Both the refraction interpretation process and the assumption that horizontal shear waves do not convert to compressional or vertical shear waves are based on the condition that the seismic line runs along the dip direction of planar boundaries. In fact, the water table near a recharge source, such as the canal, slopes up toward the source; therefore, this survey was along a line normal to the dip direction. Based on data from a test spread that ran normal to the canal through the survey area, the dip on the boundary of interest was approximately 8 deg, sloping up toward the canal. Because the velocities and depths from the test spread were close to the values obtained from the survey parallel to the canal, this small dip angle apparently did not introduce serious error into the interpretation process.

Area 2 refraction results

41. The seismic refraction survey in Area 2 was conducted as an example of an additional application of this method. The reflection seismic crews required information about the shallow structures in the area for use in static corrections.* In places, layers with compressional velocities similar to those expected at a water table were detected from a previous refraction line. A comparison of V_p to V_s was required to determine if this layer represented water saturation or weathered bedrock.

42. Analysis of the time-distance curves resulted in the apparent velocities shown in Table 3. The velocity-depth model shown in Figure 7 is the result of computer-assisted analyses of these data. The low compressional velocity in the third layer and the marked decrease in the V_p/V_s ratio as shown in Figure 7 are probably not indicative of a water table. In the fourth layer, V_p is somewhat high for a water table and V_p/V_s is low, having

* Corrections applied to seismic data to compensate for the effects of variations in elevation, weathering thickness, weathering velocity, or reference to a datum.

Table 3

Area 2 Apparent Velocities and Intercept Times

(Velocities in feet per second,

Times in milliseconds)

Spread	Layer	Northeast velocity, t_0	Southwest velocity, t_0
901-908,P	1	833	714
	2	2,453, 8	2,541, 12
	3	4,062, 14	4,193, 15
	4	9,167, 27	8,250, 24
907-908,S	1	385	417
	2	750, 10	750, 10
	3	2,766, 35	3,421, 45
	4	6,111, 56	
908-909,P	1	714	667
	2	3,611, 12	4,000, 11
	3	8,667, 24	8,250, 22
908-909,S	1	312	333
	2	1,250, 25	1,204, 21
	3	3,714, 40	3,513, 32
	4	6,111, 56	7,333, 45

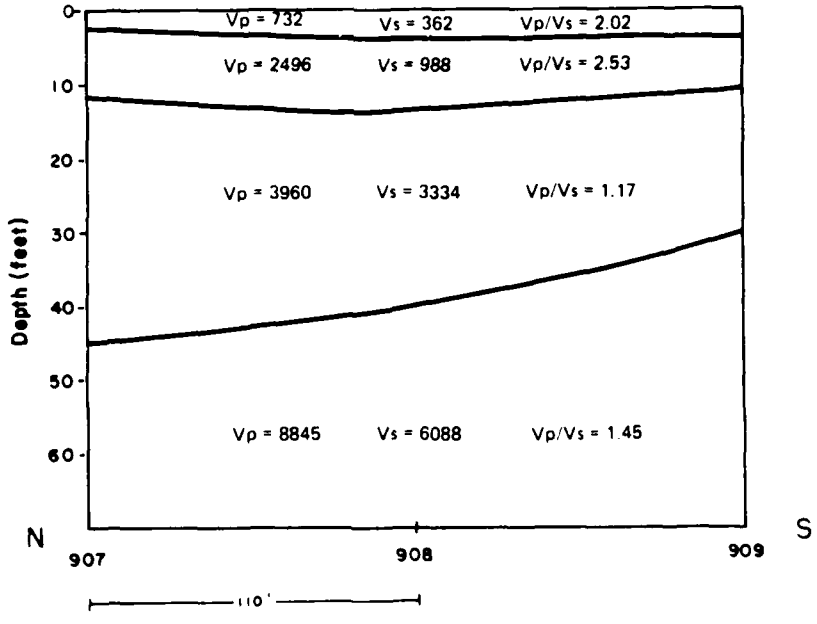

Figure 7. Area 2 velocity profile (velocities in feet per second)

increased only 24 percent over the value in the layer above. Because a shallow water table is not likely to exist in the geologic conditions present at this site, these results are as expected.

PART V: CONCLUSIONS AND RECOMMENDATIONS

Conclusions

43. The following conclusions can be drawn from this study:

a. The hammer source, used with a digital seismograph capable of reversing the polarity and stacking the signal from several hammer blows, is capable of consistently generating good quality horizontal shear wave first arrivals to a distance of 330 ft in the geologic settings under which tests were conducted. The major limitation of this type of source is the low signal strength and thus the limited depth of investigation that can be achieved.

b. This preliminary investigation indicates the feasibility of distinguishing between a lithologic boundary and a water table, using the comparison of V_p to V_s in conjunction with lithologic information.

Recommendations

Equipment

44. To stack reversed polarity shear wave signals in the field, a rugged portable seismograph capable of easily reversing the polarity of incoming signals and storing the stacked traces in memory is necessary. Such a system would be required for use in a tactical environment. Several digital signal-enhancement portable seismographs that meet these requirements are now commercially available. In addition, a 24-channel rather than 12-channel system would allow greater depths of investigation while still providing adequate resolution of velocity layers.

Data processing and interpretation

45. The ideal system to use would be a compatible microcomputer and seismograph pair that would allow field records to be stored directly onto a diskette for later processing with the aid of microcomputer programs. The next best system would consist of a compatible tape recorder and seismograph pair, as used in this study, with appropriate software to transfer the records from a tape to a diskette for use with a microcomputer.

46. Although computer programs are being developed to pick first arrival times or to fit apparent velocity lines to time-distance plots, these programs are not sufficiently sophisticated to be reliable, especially when

the records are noisy or the subsurface geology is not ideally simple. While the seismic traces could be displayed and amplified on a computer screen to facilitate picking, the actual travel time picks should be made by a trained individual. To obtain the best results from the data, the apparent velocity analysis should be performed by an individual experienced in the interpretation of seismic refraction data and familiar with the general geology of the survey area.

47. After the time picks and apparent velocity analysis have been completed, computer programs for analysis of multiple dipping layers could be used to arrive at a model of the depths and dips of various velocity layers. A program that assumes planar layers would be adequate for the majority of geologic situations in which shallow water table aquifers are found. Such a program, however, would be misleading in those cases where severely irregular surfaces occur between velocity layers within a single spread length.

Personnel

48. A person trained and experienced in refraction interpretation, preferably someone with a geoscience background, would be needed to check the travel time picks, perform the apparent velocity analysis, and assist with the final interpretation of the data. However, the field crews who conduct the surveys and collect the data could be composed of technically trained, non-degree personnel. The training program for the field crews should cover the following topics:

a. Operation and simple maintenance of seismographs, geophones, cables, and sources.

b. Layout of seismic refraction lines, including proper geophone planting and noise-reduction techniques.

c. Recognition of expected wave shapes and first arrivals so that travel time picks could be made in the field.

d. Recognition of records of unacceptable quality to determine if any repeat measurements are required.

US Army Terrain Team personnel could easily handle this task with the above training.

Future studies

49. Because many water tables of interest are more than 50 ft below the ground surface, a stronger source would be required for widespread application of this method. Stumpel et al. (1984) reported using a hydraulically driven hammer-type shear source with spread lengths of up to 1,640 ft. Shear

waves can also be generated with explosives (Omnes 1978) by drilling three shot holes at each shot point. The center hole is shot for compressional waves, and then the hole on one side is shot for shear wave generation. The disrupted material around the center hole transmits motion poorly, resulting in motion in the direction away from the center and a polarized SH wave propagating normal to the line of the three shot holes. The other side hole is then shot for reversed polarity SH. This method has the disadvantage of requiring the drilling or digging of numerous shot holes, often in poorly consolidated gravelly material in which drilling is slow and holes tend to collapse. However, developing explosive shear sources could be necessary when very deep water tables are investigated.

50. From the results obtained in this survey, compressional velocity appears to increase at a rate greater than that of shear wave velocity at a water table. To confirm these observations, future investigations should include well site data. In addition, longer spread lengths and greater overlaps of adjacent spreads could provide more information about deeper water tables. Finally, research on clay-bearing aquifers for which the capillary fringe is much thicker than in sandy aquifers, and research on deep water tables where the contrast between saturated and unsaturated compressional wave velocities is minimized, should help to define the useful limits of this method of water table detection.

51. Expert systems, which incorporate the knowledge of human experts with data base information and artificial intelligence decision logic, would lend themselves well to the interpretation of V_p/V_s data in a tactical environment. Such an expert system, the "Water Resources Advisor," currently being developed under contract to WES, will be a powerful tool available for identifying potential subsurface water resources in a tactical environment.

REFERENCES

Applegate, J. K. 1974. "A Torsional Seismic Source," Ph.D. Dissertation, Colorado School of Mines, Golden, Colo.

Biot, M. A. 1956. "Theory of Propagation of Elastic Waves in a Fluid Saturated Porous Solid, I: Low Frequency Range," Journal of the Acoustical Society of America, Vol 28, pp 168-178.

Eaton, G. P. 1974. "Seismology," Application of Surface Geophysics to Ground-Water Investigations, USGS Tech. Water-Resources Inv., Book 2, Chap. D1, pp 67-84.

Freeze, R. A., and Cherry, J. A. 1979. Groundwater, Prentice-Hall, Inc., Englewood Cliffs, N. J.

Gibson, J. B., Boomer, D. R., and Schoellhorn, H., III. 1979. "Bi-directional Impulse Shear Wave Generator and Method of Use," US Patent No. 4,301,888, C 81.11.24, F 79.10.17 (Appl 85,566) (Chevron Research).

Kuster, G. T., and Toksoz, M. N. 1974. "Velocity and Attenuation in Two Phase Media," Geophysics, Vol 39, pp 587-606, 607-618.

Levshin, A. L. 1961. "Determination of Ground Water Level by the Seismic Method," Akad. Nauk. SSSR Izu. Ses. Geofiz, No. 9, pp 857-870.

Mooney, H. M. 1984. Handbook of Engineering Geophysics, Vol 1: Seismic, Bison Instruments Inc., Minneapolis, Minn.

Omnes, G. 1978. "Exploring with SH-waves," Journal of the Canadian Society for Exploration Geophysics, pp 40-49.

Stumpel, H., Kahler, S., Meissner, R., and Mikereit, B. 1984. "The Use of Seismic Shear Waves and Compressional Waves for Lithological Problems of Shallow Sediments," Geophysical Prospecting, Vol 32, pp 662-675.

White, J. E. 1983. Underground Sound-Application of Seismic Waves, Elsevier Science Publishers B.V., Amsterdam, The Netherlands.

White, J. E., and Sengbush, R. L. 1953. "Velocity Measurements in Near-surface Formations," Geophysics, Vol 18, pp 54-69.

Won, I. J. 1980. "Torsional Shear Wave Generator," US Patent No. 4,303,666, C 82.01.12, F 80.02.22 (Appl 123,651).

APPENDIX A: UNCONSOLIDATED GRANULAR MEDIUM MODEL*

* The description of variations in seismic compressional velocity V_p and shear wave velocity V_s due to water saturation of an unconsolidated granular medium is paraphrased from the model described by Levshin (1961) and White and Sengbush (1953).

1. Unconsolidated granular media can be modeled by ideally elastic spheres in a simple cubic packing arrangement and under the pressure of their own weight. The P-wave velocity V_p^a when the pores between spheres are completely void is given by

$$V_p^a = \left\{ \frac{5.78}{\rho(1 - \eta)} \left[\frac{E^2 \rho z}{\left(1 - \sigma^2\right)^3} \right]^{\frac{1}{3}} \right\}^{\frac{1}{2}} \tag{A1}$$

in which ρ is density, η is the porosity, E is Young's modulus, z is depth from the surface, and σ is Poisson's ratio. For cubic packing of spheres, $\eta = 0.476$. When z is more than 1.6 ft, this equation can be used even when the pore space is filled with air at atmospheric pressure.

2. The velocity of shear waves is given by

$$V_s^a = \left\{ \frac{3.41(1 - \sigma)}{\rho(1 - \eta)} \left[\frac{E^2 \rho z}{\left(1 - \sigma^2\right)^3} \right]^{\frac{1}{3}} \right\}^{\frac{1}{2}} = \sqrt{\frac{\mu}{\rho(1 - \eta)}} \tag{A2}$$

in which μ is the shear modulus. When air in the pore space is replaced by water, μ remains unchanged, while the density of the medium increases. Given the values of the densities of air or water at atmospheric pressure, shear velocity in the saturated medium should not vary by more than 15 percent from the shear velocity in the totally dry medium.

3. If the pores are all air filled to a depth h_w and completely water filled below that depth, the velocity variations that can be expected are described below:

a. $z < h_w$. The mean velocity along a vertical path to depth z is $V_s^a = \dfrac{Z}{\int_0^z \frac{dz}{V(z)}} = 5/6\ V_p(z)$ where $V(z)$ is a function describing the change in V_p with depth, and $V_p(z)$ is the value of V_p at a particular depth z. By this same relationship, $V_s^a = 5/6 V_{s(z)}$. The ratio of V_p to V_s above the water saturation

level is $V_p^a/V_s^a = 1.3/(1 - \sigma)^{0.5}$ and depends only on Poisson's ratio.

b. $z > h_w$. The compressional velocity below the water line is affected by the elasticity of the water and is described by:

$$V_p^b = \frac{\left\{ \frac{1}{\frac{\eta}{k_l} + \frac{1 - \eta}{k}} + 5.78 \left[\frac{E^2(\rho - \rho_l) + \rho_l h_w}{(1 - \sigma^2)^3} \right]^{\frac{1}{3}} \right\}^{\frac{1}{2}}}{\left[\rho(1 - \eta) + \rho_l \eta \right]^{\frac{1}{2}}} \qquad \text{(A3)}$$

in which k is the bulk modulus of the spheres, k_l is the bulk modulus of the liquid, and ρ_l is the density of the liquid. Below the water level, the effective density is $\rho_b = (1 - \eta)\rho + \eta\rho_l$ and the shear wave velocity is

$$V_s^b = \left\{ \frac{3.41\ (1 - \sigma)}{\rho(1 - \eta) + \rho_l \eta} \left[\frac{E^2(\rho - \rho_l) + \rho_l h_w}{(1 - \sigma^2)^3} \right]^{\frac{1}{3}} \right\}^{\frac{1}{2}} \qquad \text{(A4)}$$

The ratio of V_p to V_s in the saturated zone is then:

$$V_p^b/V_s^b = V_p^a/V_s^a \left[1 + \frac{\left(\frac{1}{\frac{n}{k_l} + \frac{1 - \eta}{k}} \right)^{\frac{1}{2}}}{\left[\frac{E^2(\rho - \rho_l)z + \rho_l h_w}{(1 - \sigma^2)^2} \right]^{\frac{1}{3}}} \right] \qquad \text{(A5)}$$

c. $z = h_w$. The term added to 1 in Equation A5 is always positive; then the V_p/V_s ratio below h_w must be greater than the ratio above h_w.

APPENDIX B: TIME-DISTANCE PLOTS AND TRAVEL TIME DATA

Area 1 P-Wave

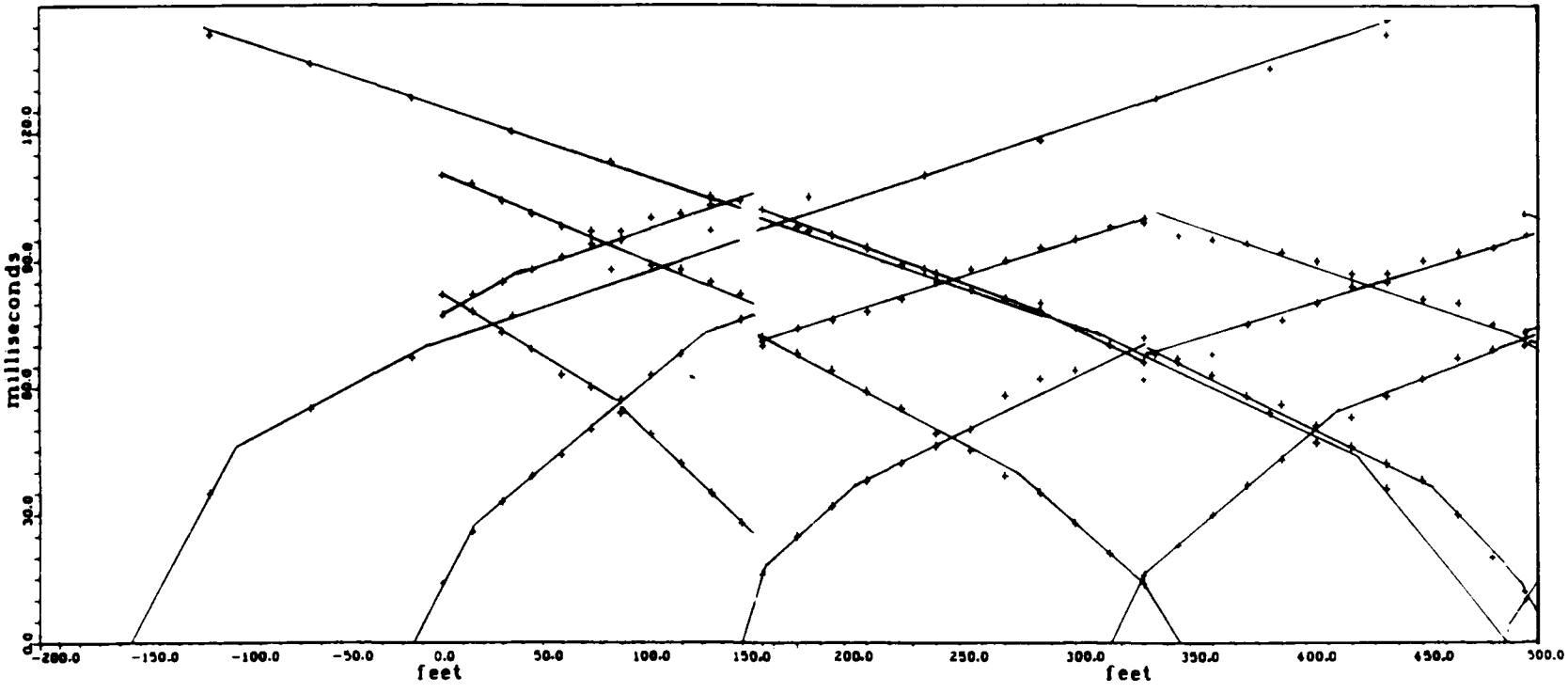

(Continued)

(Sheet 1 of 2)

Area 1 P-Wave

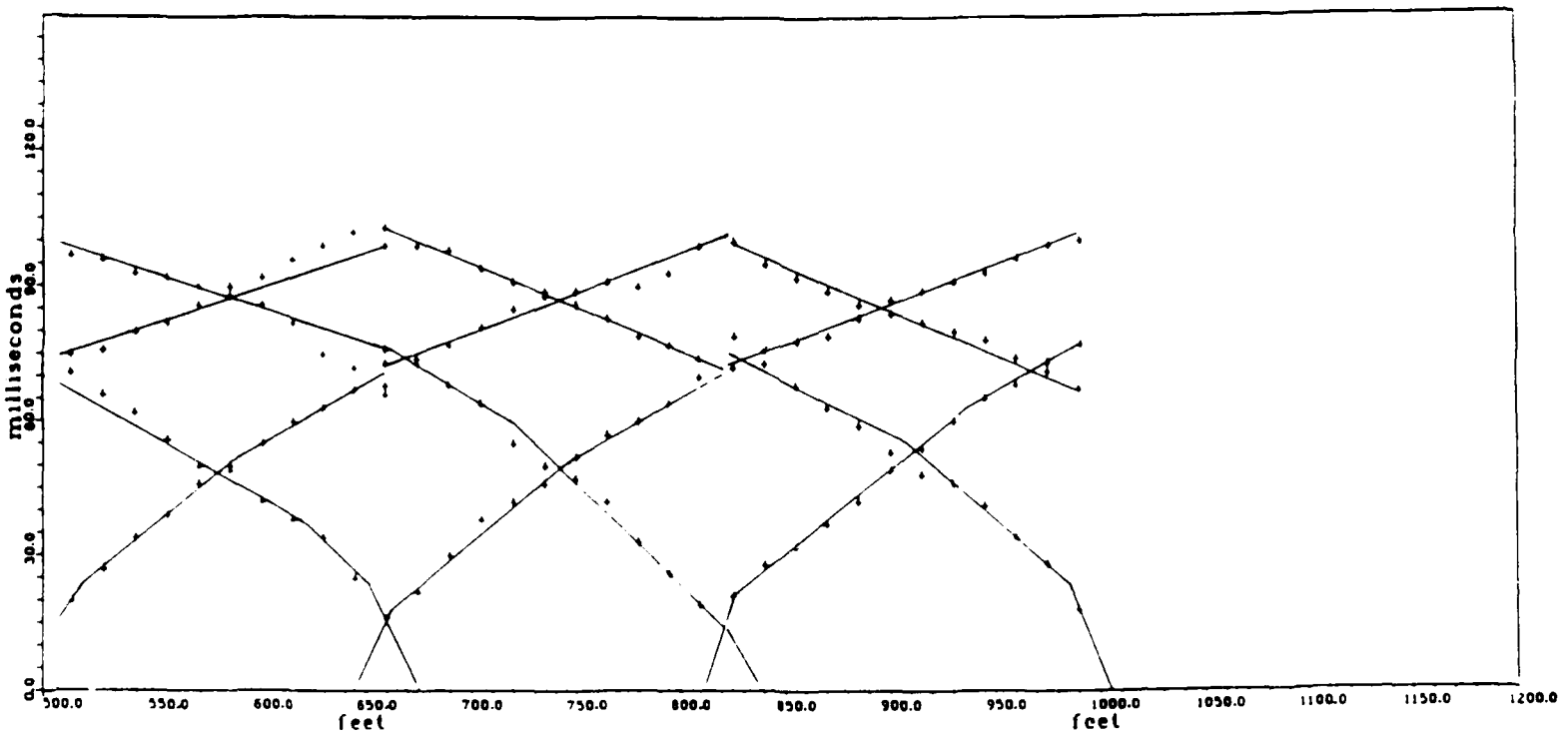

(Concluded)

(Sheet 2 of 2)

Area 1 S-Wave

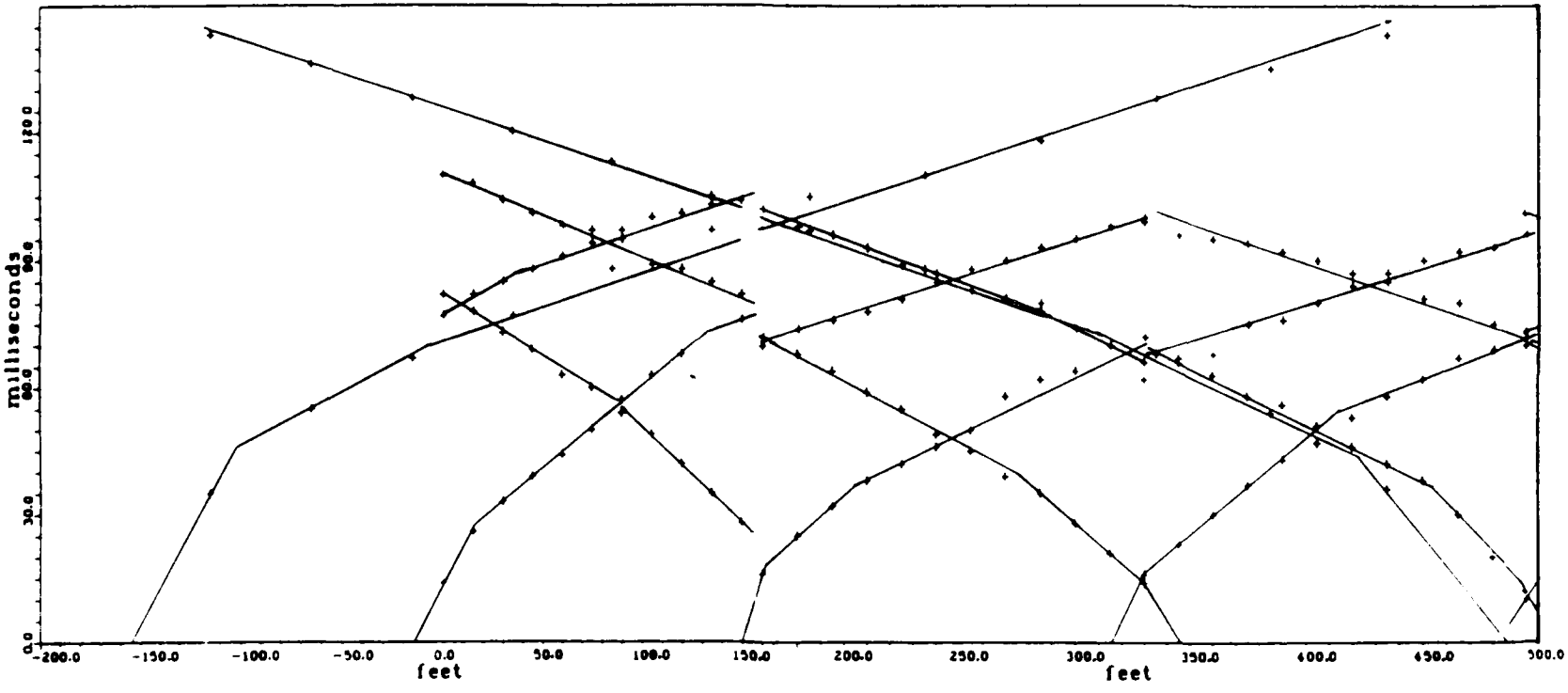

(Continued)

(Sheet 1 of 2)

Area 1 S-Wave

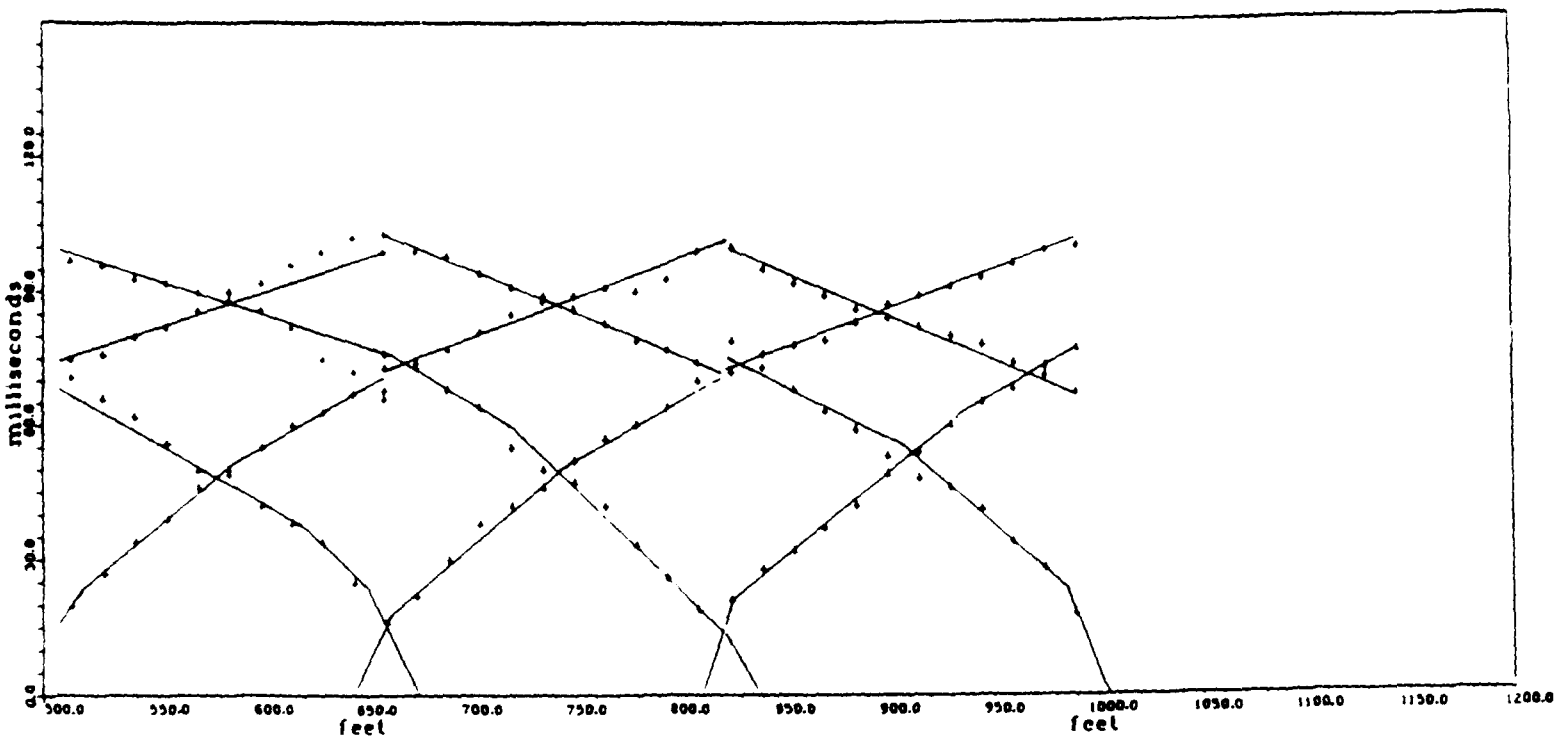

(Concluded)

(Sheet 2 of 2)

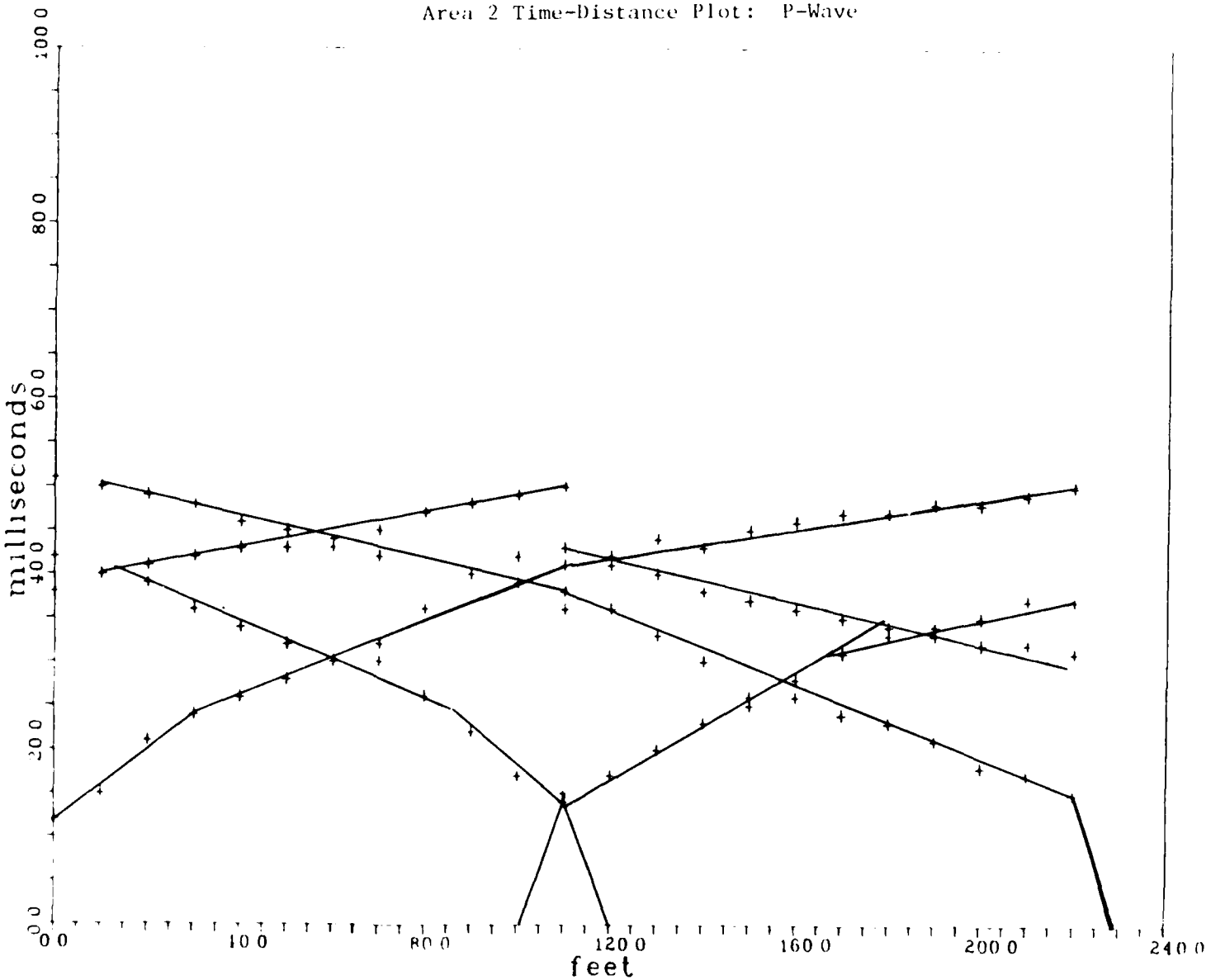
Area 2 Time-Distance Plot: P-Wave
milliseconds
0.0
20.0
40.0
60.0
80.0
100.0
0.0
40.0
80.0
120.0
160.0
200.0
240.0
feet

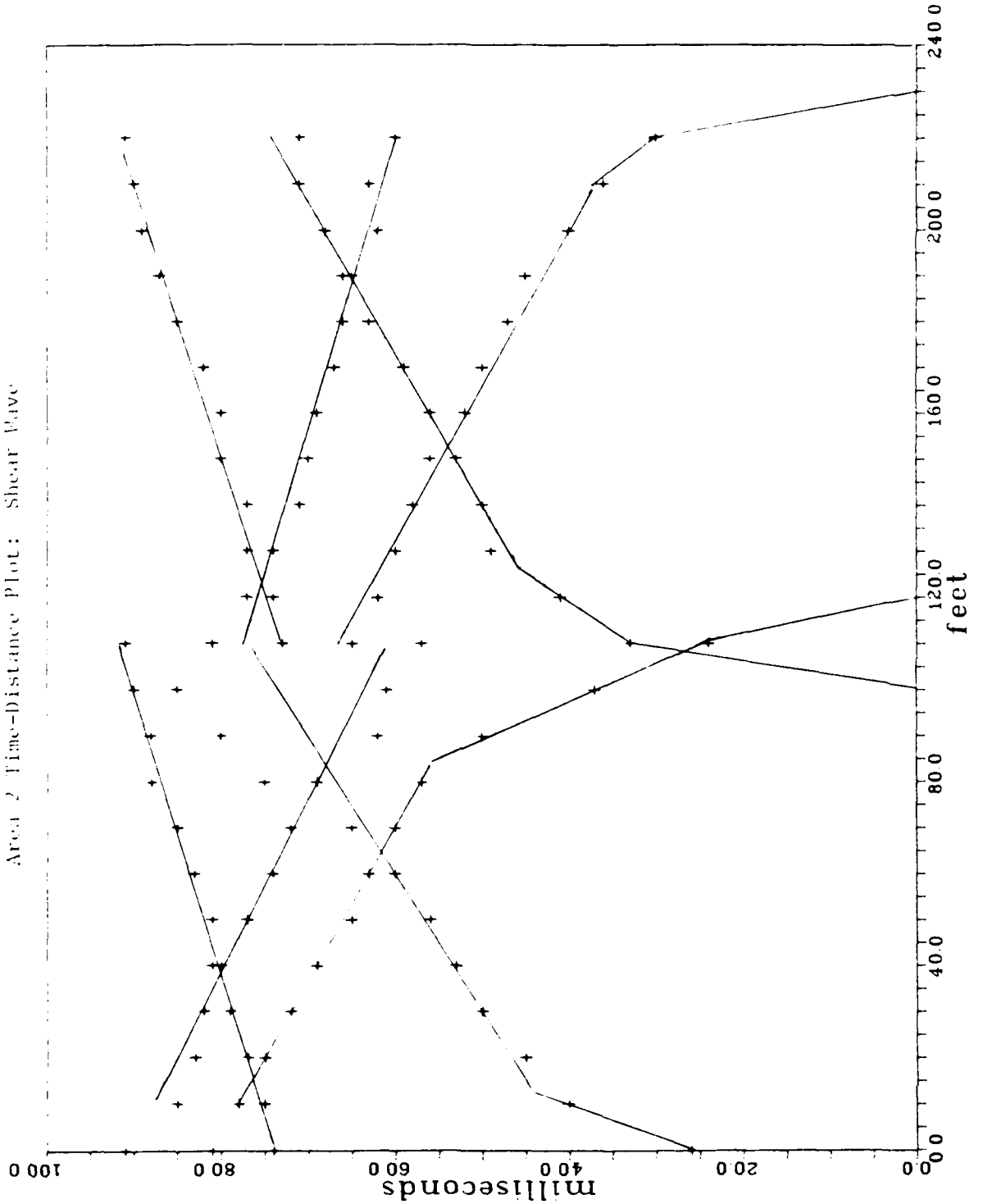
Area 2 Time-Distance Plot: Shear Wave
milliseconds
0.0
20.0
40.0
60.0
80.0
100.0
feet
0.0
40.0
80.0
120.0
160.0
200.0
240.0

Travel Time Data - Area 1*

Mode*	Source Station	Geophone Station											
		0	15	30	45	60	75	90	105	120	135	150	165
S	-165		135	145	151	157	163	171	180	187	194	200	
	-15	23	45	55	64	72	79	90	101	109	116	120	126
	180				114	103	84	75		63	51	40	25
	330	200	196	187	180	176	170	165	160	152	145	139	134
P	-165	77	82	85	88	91	94	97	100	101	103	104	106
	-15	14	26	33	39	44	50	57	63	68		76	78
	180	82	78	73	69	63	60	54	49	42	35	28	20
	330	110	108	104	101	98	97	95	89	88	85	82	78
		165	180	195	210	225	240	255	270	285	300	315	330
S	0	126	130	135	140	148	154	159	164	170	176	184	188
	150	24	46	52	64	80	88	94	95	107	112	119	125
	345	120	118	110	100	94	84	73	64	61	49	37	25
	495	183	180	171	158	156	149	144	136	133	128	120	115
P	0	70	74	76	78	81	85	88	90	93	95	98	100
	150	16	25	32	38	42	46	50	58	62	64	70	72
	345	72	68	64	59	55	49	45	39	35	28	21	14
	495	102	98	96	93	89	87	83	81	78	74	70	66
		330	345	360	375	390	405	420	435	450	465	480	495
S	165	108	115	115	128	136	143	148	154	163	165	176	180
	315	28	42	54	63	71	81	86	97	105	110	116	117
	510	122	112	102	100	92	86	85	75	70	55	36	18
	660	190	185	171	173	167	160	155	146	142	137	131	121
P	165	62	66	68	75	76	80	84	87	90	92	93	96
	315	16	23	30	37	43	47	53	58	62	67	69	72
	510	72	67	63	58	56	51	46	42	38	30	20	12
	660	99	96	95	94	92	90	87	85	81	80	75	71
		495	510	540	525	540	555	585	600	615	630	645	660
S	330	118	124	129	138	141	152	159	168	172	180	189	194
	480	21	44	60	71	73	80	88	101	110	116	122	130
	675	129	124	112	106	95	87	77	70	68	59	45	25
	825	200	190	183	179	172	161	152	150	146	140	130	120
P	330	70	75	76	80	82	86	90	92	96	99	102	103
	480	10	20	27	34	39	46	50	55	60	63	67	73
	675	73	71	66	62	56	50	49	42	38	34	25	16
	825	101	97	96	93	92	90	88	86	82	75	72	66

(Continued)

* Station locations are expressed in feet; times, in milliseconds.

** P = compressional wave; S = shear wave.

Area 1 (Concluded)

Mode*	Source Station	Geophone Station											
		660	675	690	705	720	735	750	765	780	795	810	825
S	495	123	133	140	150	156	160	163	170	179	184	190	200
	645	30	41	54	64	78	82	85	90	103	116	122	130
	840	135	129	121	110	99	88	77	77	63	56	45	30
	990	197	191	182	177	170	164	163	150	141	137	130	127
P	495	68	73	77	81	85	88	89	91	90	93	99	102
	645	16	22	30	38	42	46	52	57	60	64	70	74
	840	76	74	68	64	55	50	47	42	33	26	19	12
	990	99	99	98	94	91	89	86	83	79	77	74	69
		825	840	855	870	885	900	915	930	945	960	975	990
S	660	126	130	134	143	145	156	163	169	173	181	185	195
	810	34	46	54	64	73	84	96	102	109	118	125	132
	1005	133	126	117	109	100	94	87	76	68	57	50	31
	1155	185	183	174	162	151	146	143	140	134	129	122	116
P	660	72	76	78	79	83	87	89	91	93	96	99	100
	810	21	28	32	37	42	49	54	60	65	68	73	77
	1005	79	73	68	63	59	53	48	46	41	34	28	18
	1155	100	95	92	89	86	84	82	80	78	74	71	67
explosive		-115	-65	-15	35	85	135	185	235	285	335	385	435
P	-165	35	55	67	77	88	97	105	110	118	128	135	143
	485	143	136	128	120	113	105	97	88	80	68	54	36

Travel Time Data - Area 2*

Mode	Source Station	Geophone Station											
		907	+10	+20	+30	+40	+50	+60	+70	+80	+90	+100	908
S	907-110	74	75	77	79	80	81	83	85	88	88	90	91
	-10	26	40	45	50	53	56	60	65	75	80	85	81
	908 +10	81	78	75	72	69	65	63	60	57	50	37	24
	+110	91	85	83	82	81	77	74	72	69	62	61	57
P	907-110	38	40	41	42	43	43	44	45	47	48	49	50
	-10	12	15	21	24	26	28	30	32	36	40	42	43
	908 +10	42	40	39	36	34	32	30	30	26	22	17	14
	+110	51	50	49	48	46	45	43	42			39	36
		908	+10	+20	+30	+40	+50	+60	+70	+80	+90	+100	909
S	908-110	73	74	77	77	80	80	82	85	87	89	90	91
	-10	33	41	49	50	53	56	59	63	66	68	71	71
	909 +10	65	62	60	58	56	52	50	47	45	40	36	30
	+110	81	77	74	71	70	69	67	66	65	62	63	60
P	908-110	41	42	44	43	45	46	47	47	48	48	49	50
	-10	15	17	20	23	25	28	31	33	34	35	37	37
	909 +10	38	36	33	30	26	26	24	23	21	18	17	15
	+110	43	41	40	38	37	36	35	34	33	32	32	31

* Station locations are expressed in feet; times, in milliseconds.

END

DATE

3-88

DTIC